Electronic Supplementary Material (ESI) for Molecular BioSystems.

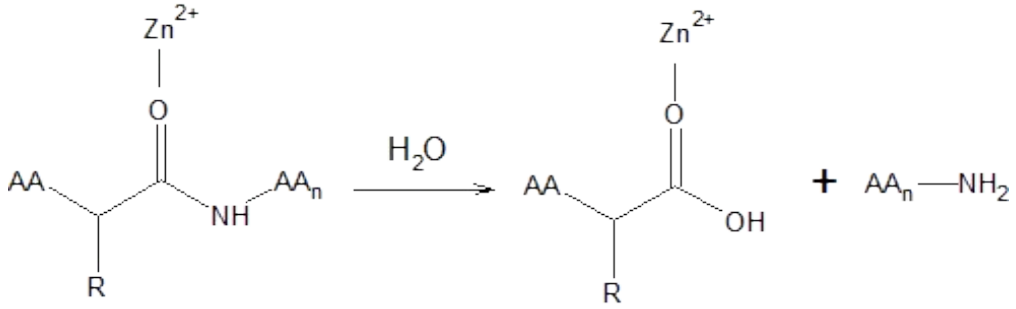

Figure S1. A schematic view of the reaction catalysed by dipeptidyl peptidase III. n=1-4.

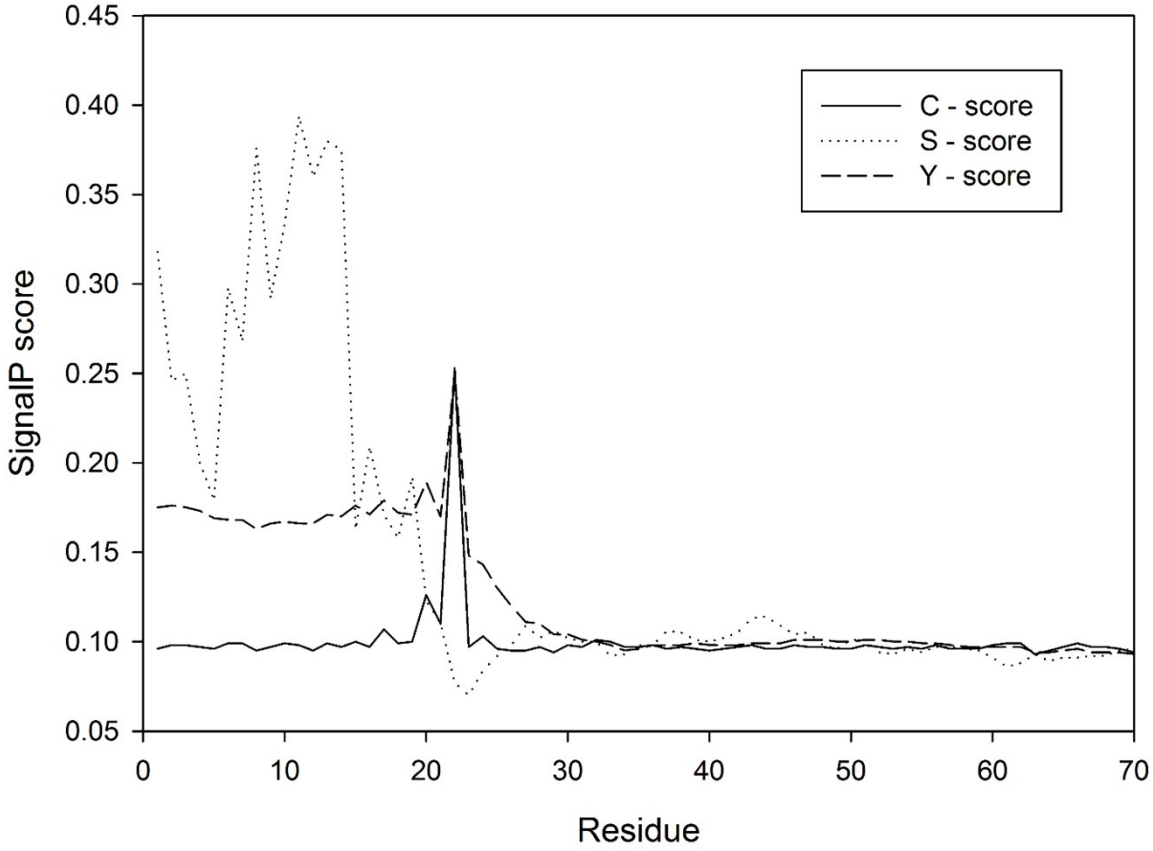

Figure S2. SignalP scores for the first 70 residues

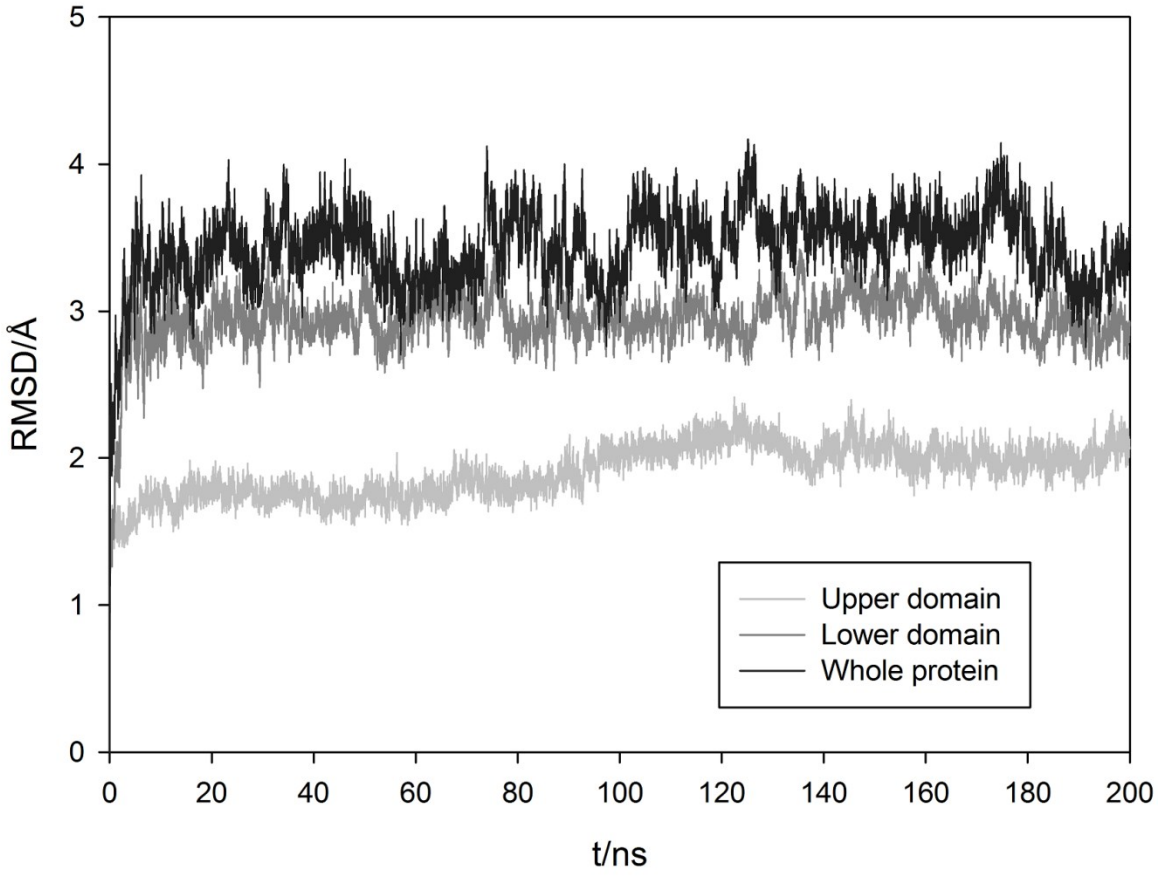

Figure S3. RMSD of the upper domain, lower domain and the whole protein over the course of 200 ns ff03 cMD simulation

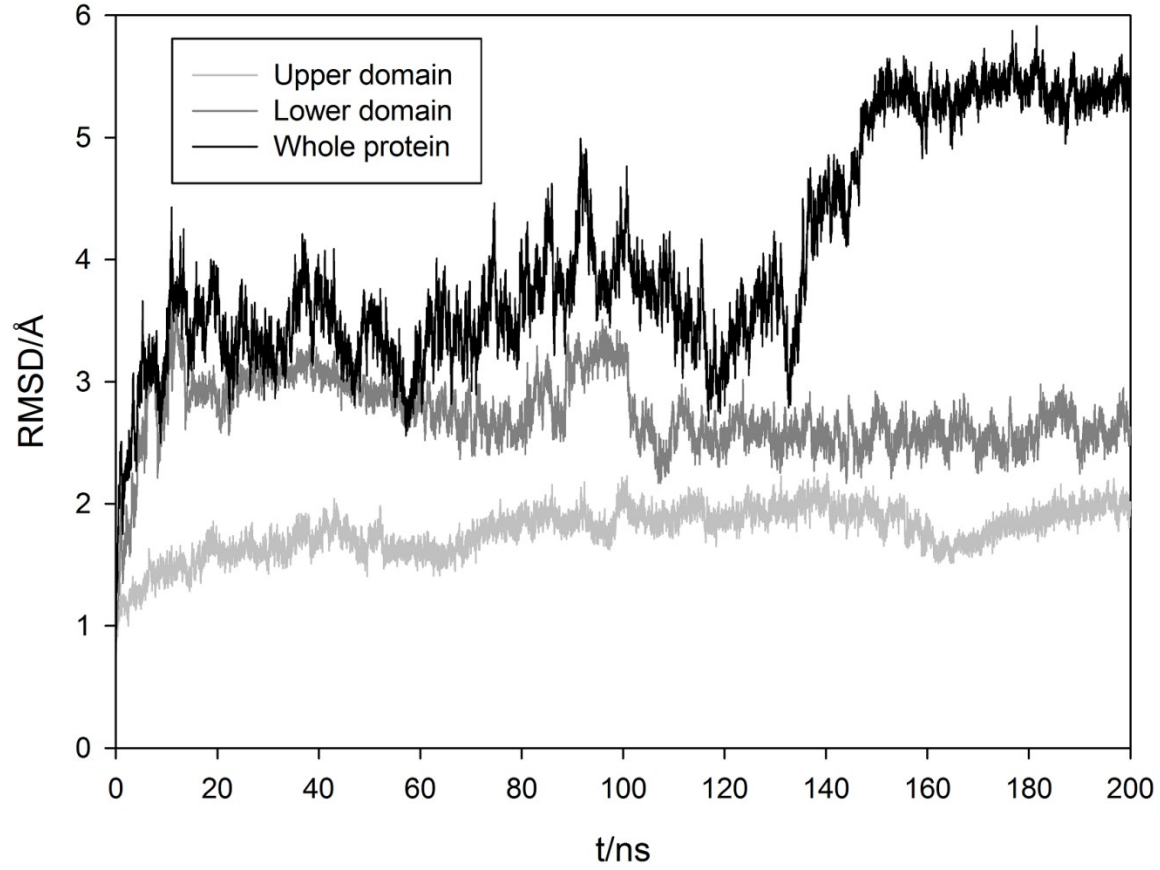

Figure S4. RMSD of the upper domain, lower domain and the whole protein over the course of 200 ns ff12SB cMD simulation

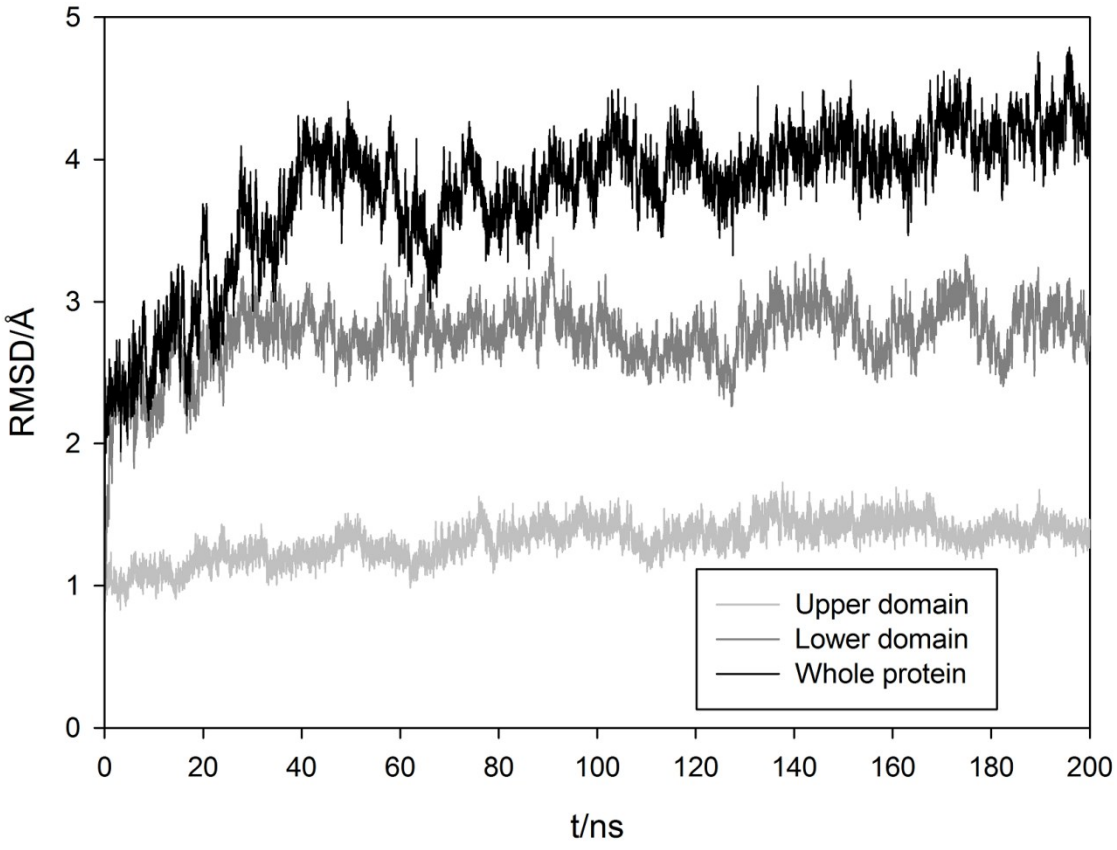

Figure S5. RMSD of the upper domain, lower domain and the whole protein over the course of 200 ns ff14SB cMD simulation

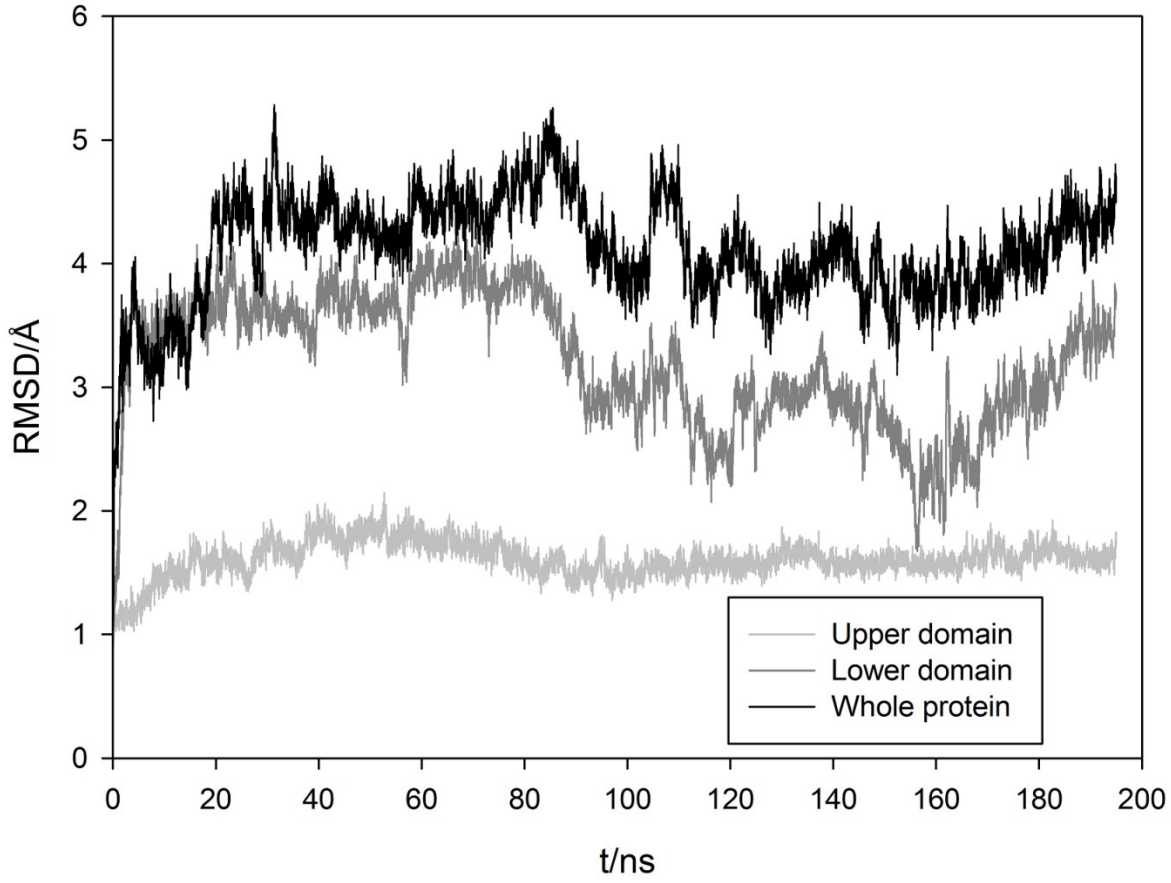

Figure S6. RMSD of the upper domain, lower domain and the whole protein over the course of 200 ns ff14SB aMD simulation

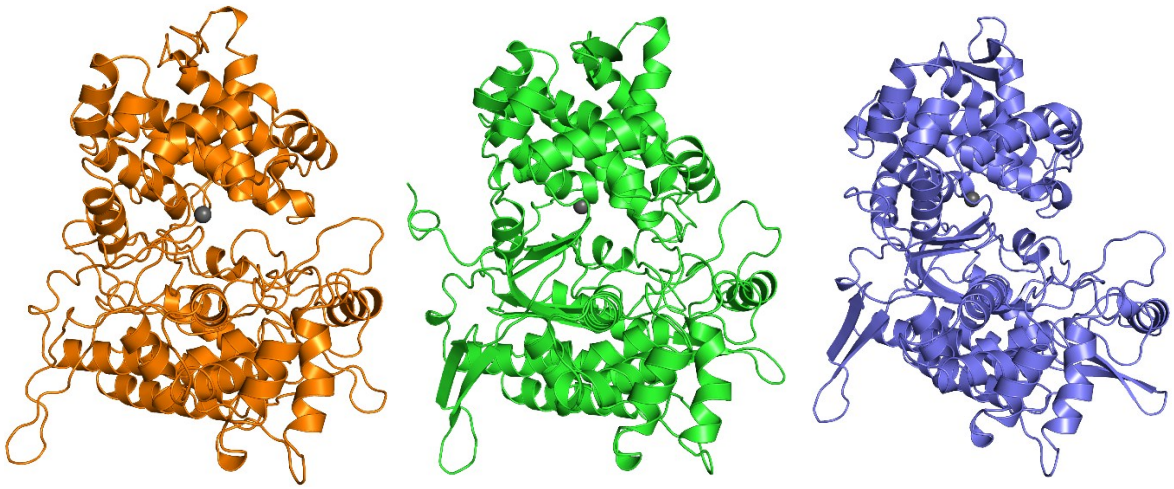

Figure S7. Crystal structure of the BtDPP III – Tris complex, cWT (left) and closed structures obtained after 200 ns of cMD-ff12SB simulations (middle) and aMD-ff14SB simulations (right)

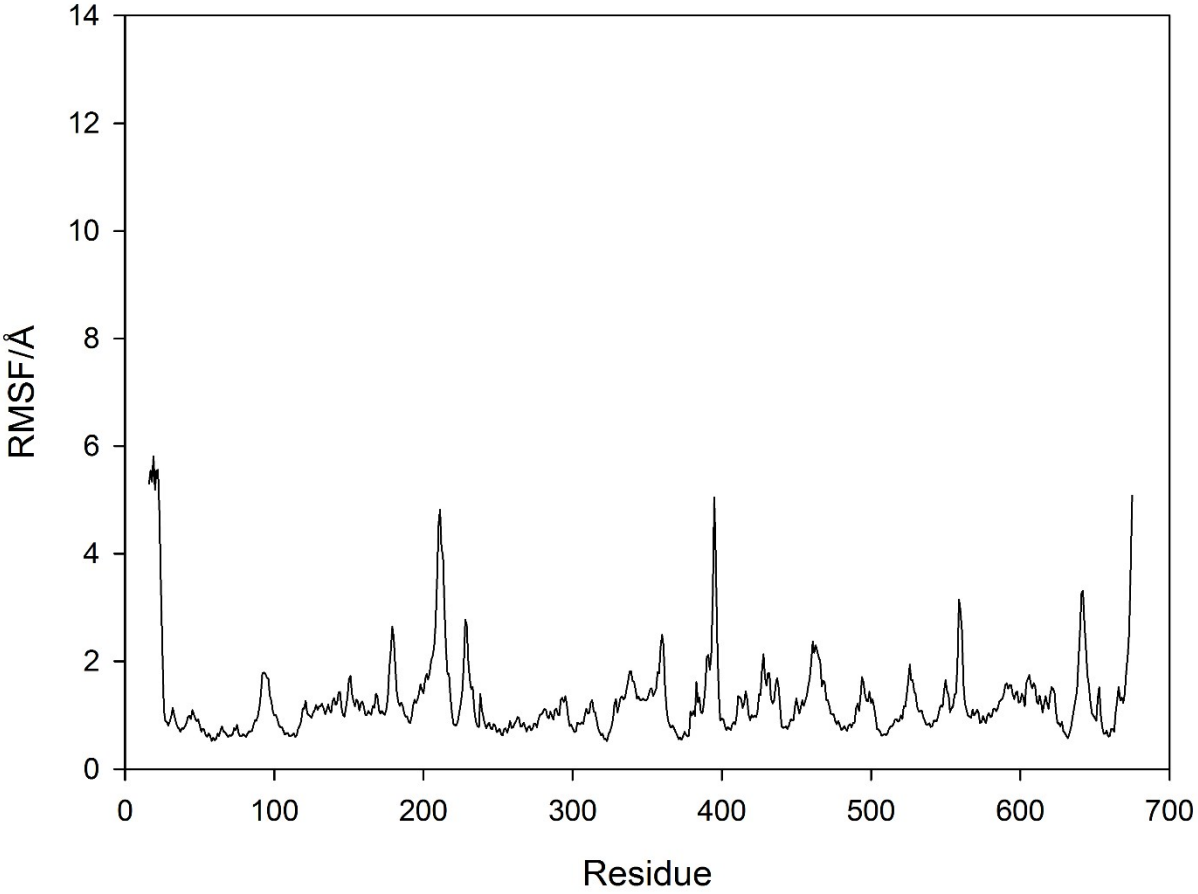

Figure S8. RMSF by residue from 200 ns of ff03 cMD simulation

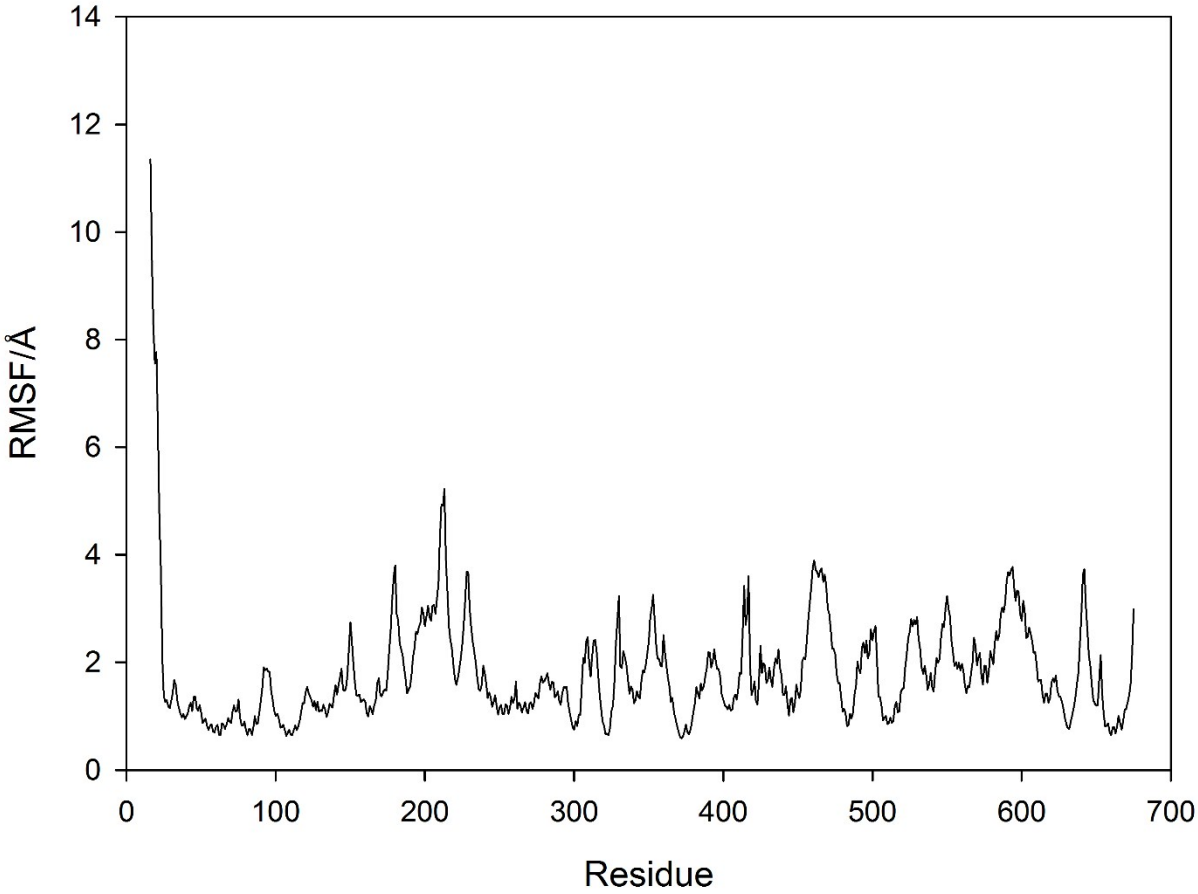

Figure S9. RMSF by residue from 200 ns of ff12SB cMD simulation

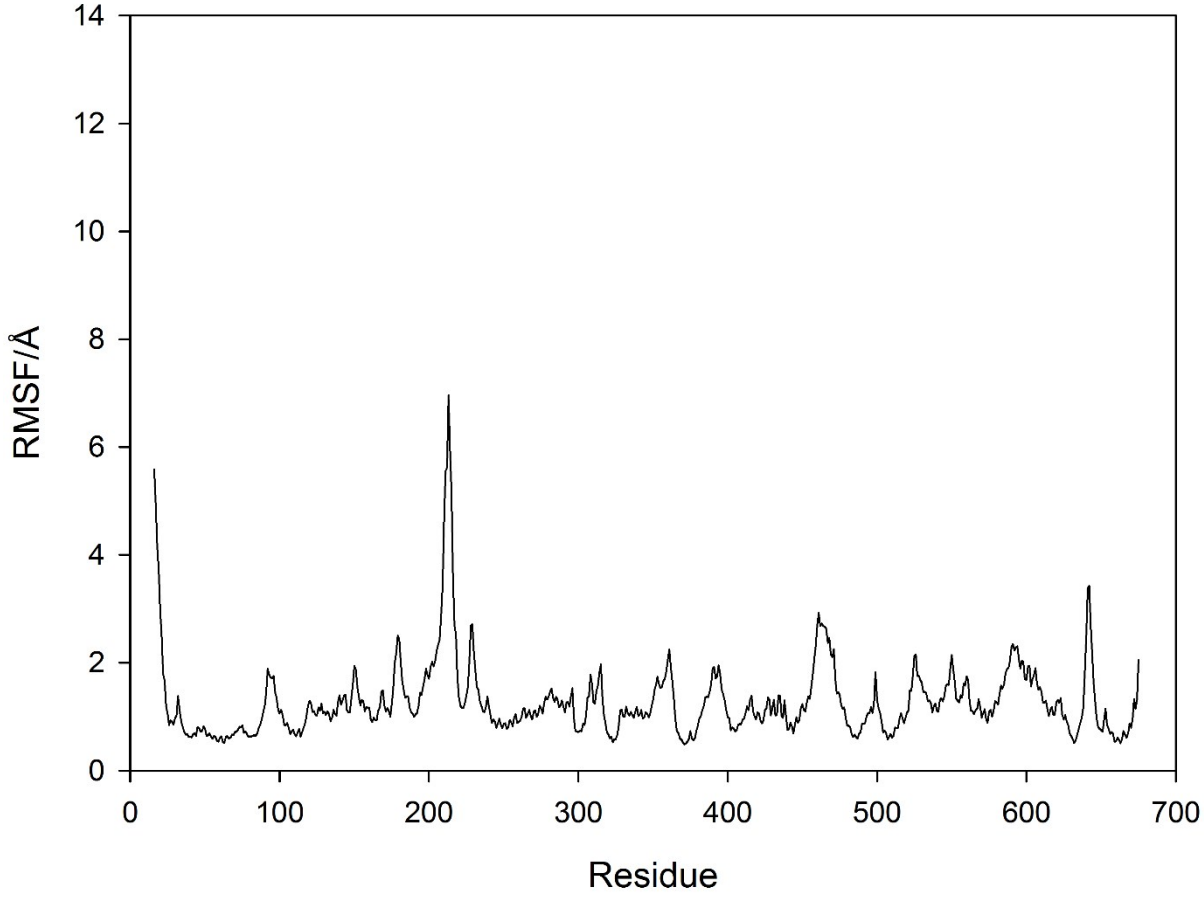

Figure S10. RMSF by residue from 200 ns of ff14SB cMD simulation

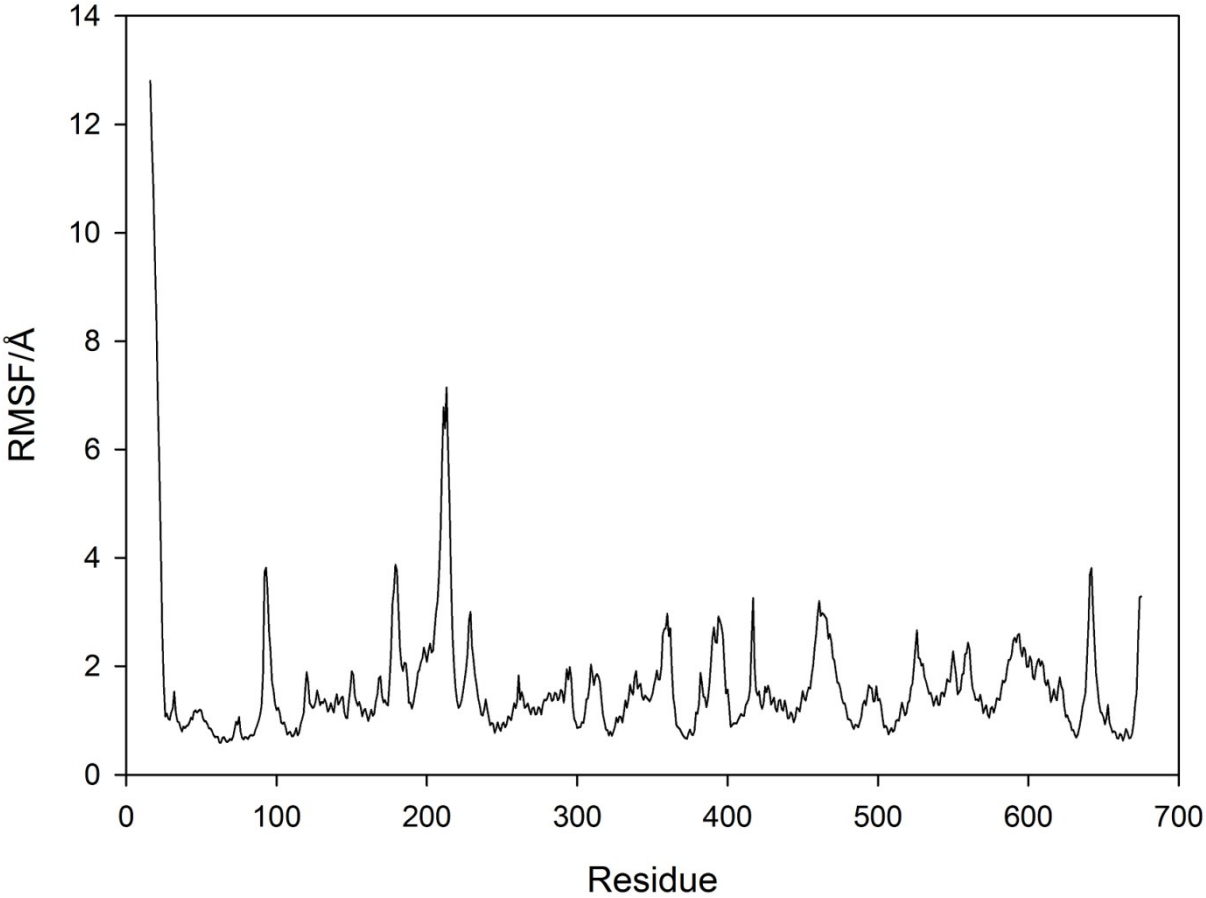

Figure S11. RMSF by residue from 200 ns of ff14SB aMD simulation

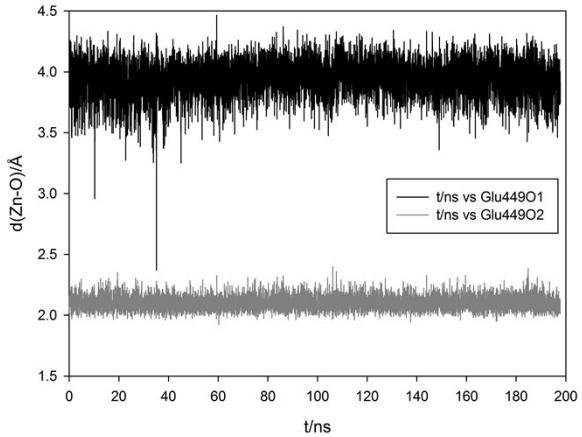

Figure S12. Distance between Zn^{2+} and the oxygen atoms of coordinating Glu449 residues over the course of 200 ns simulations of BtDPP III using ff14SB force field and accelerated MD

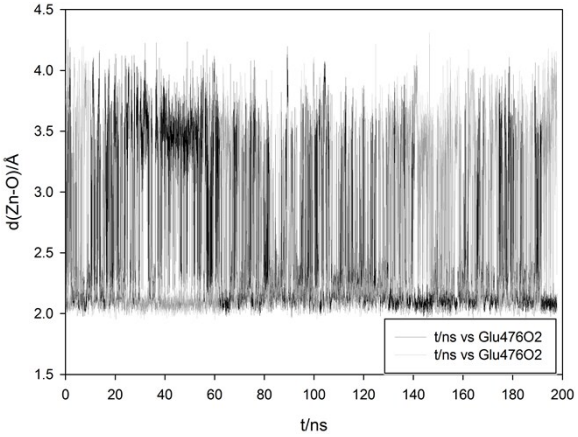

Figure S13. Distance between Zn^{2+} and the oxygen atoms of coordinating Glu476 residues over the course of 200 ns simulations of BtDPP III using ff14SB force field and accelerated MD

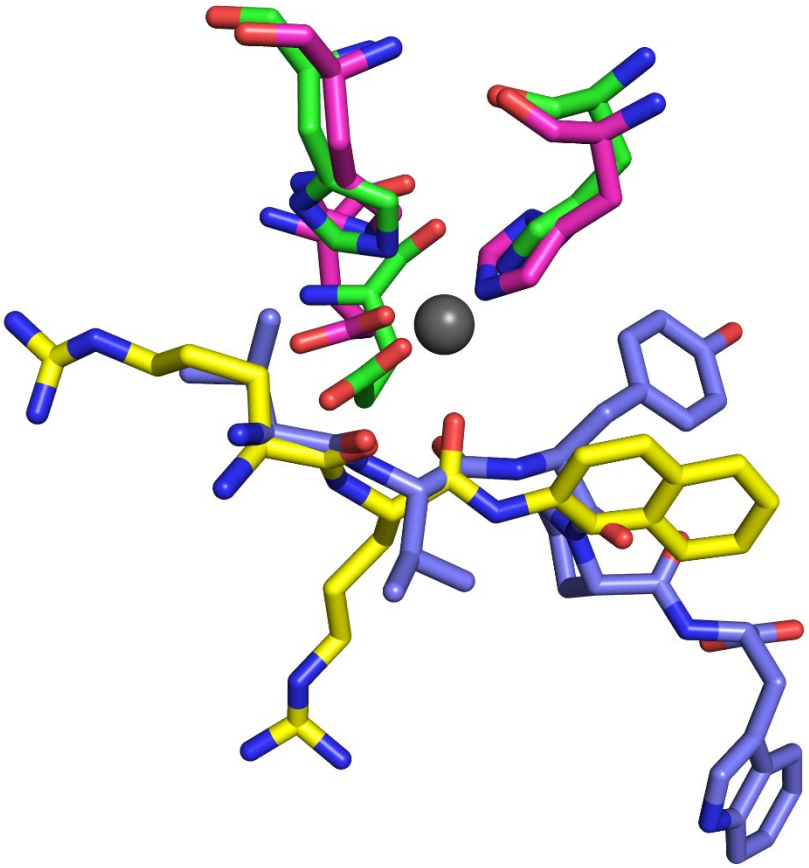

Figure S14. Overlap of active sites of crystallographically determined hDPP III – tynorphin complex structure and constructed BtDPP III – RRNA complex. Two histidines (H448 and H453 in Bt; H450 and H455 in human) and a glutamate (E476 in Bt; E508 in human) coordinating Zn^{2+} are shown. Tynorphin is shown with blue C atoms; RRNA with yellow. Zinc ion is depicted by a grey sphere.

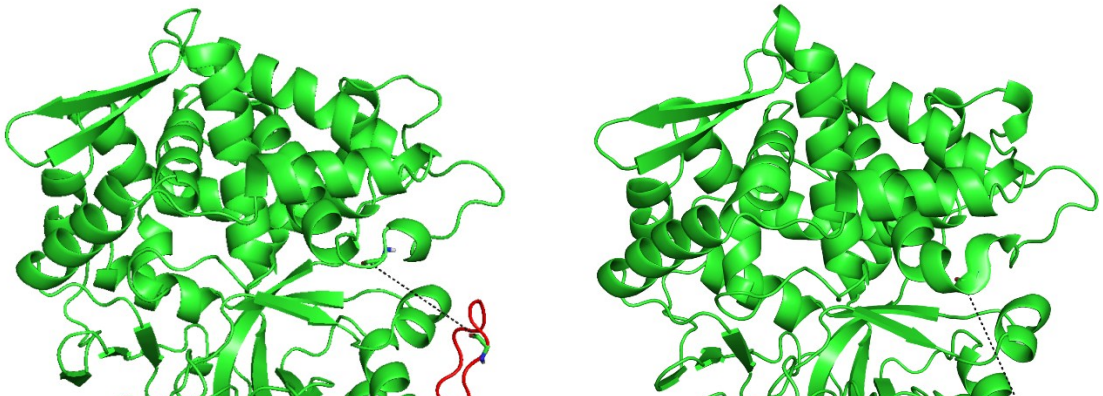

Figure S15. Translocation of the Gly204 – Tyr217 loop (higlighted in red)

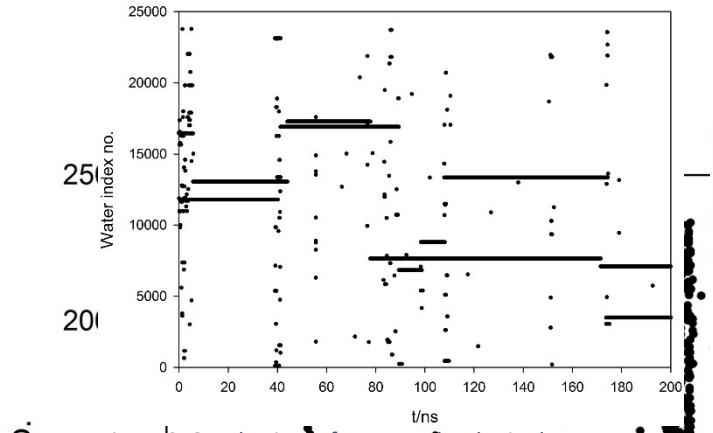

Figure S16. Behaviour of water molecules in the BtDPP III active site and close to it during 200 ns of MD simulations of the BtDPP III – RRNA complex : a) "Resistance time" for the water molecules coordinating Zn^{2+} in the BtDPP III – RRNA complex during 200 ns of ff12SB cMD simulation

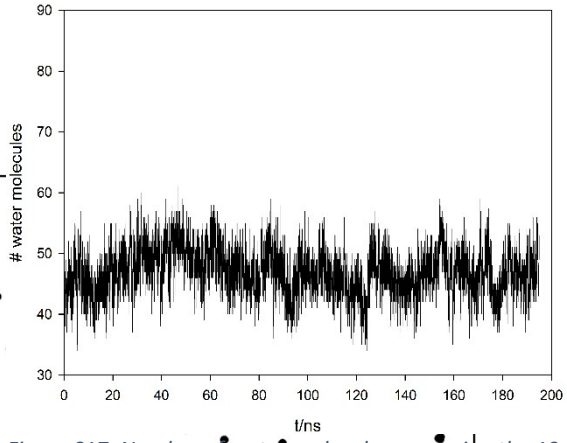

Figure S17. Number of water molecules occupying the 10 Å sphere around Zn^{2+} in the BtDPP III – RRNA complex over the course of the 200 ns of ff12 cMD simulation

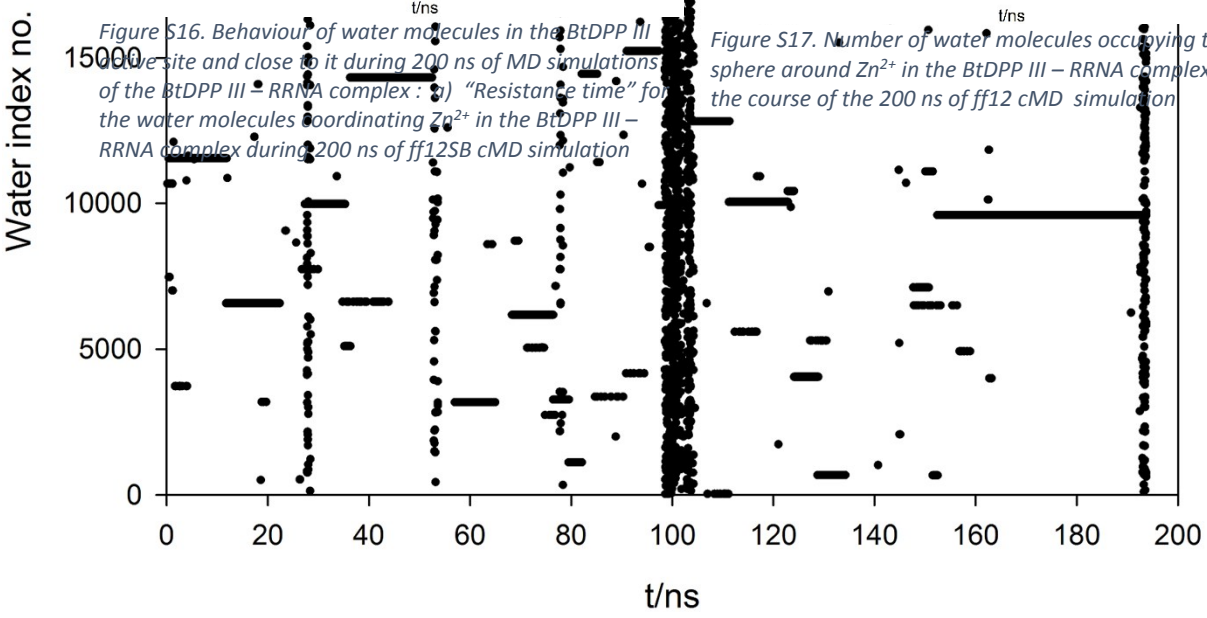

Figure S18. "Resistance time" for the water molecules coordinating Zn^{2+} in the BtDPP III – RRNA complex during 200 ns of ff14SB aMD simulation

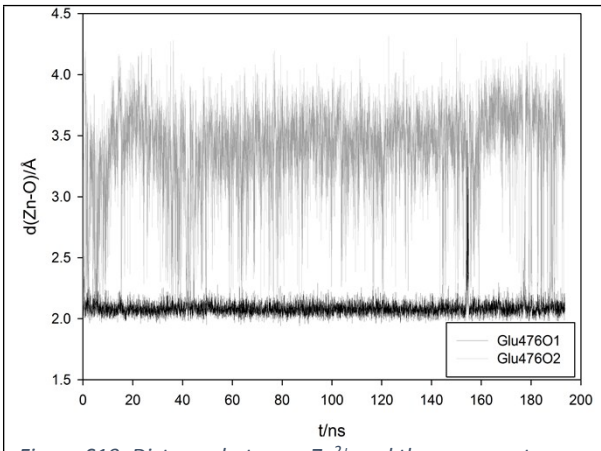

Figure S19. Distance between Zn^{2+} and the oxygen atoms of coordinating Glu476 residues over the course of 200 ns BtDPP III – RRNA complex using ff14SB force field and accelerated MD

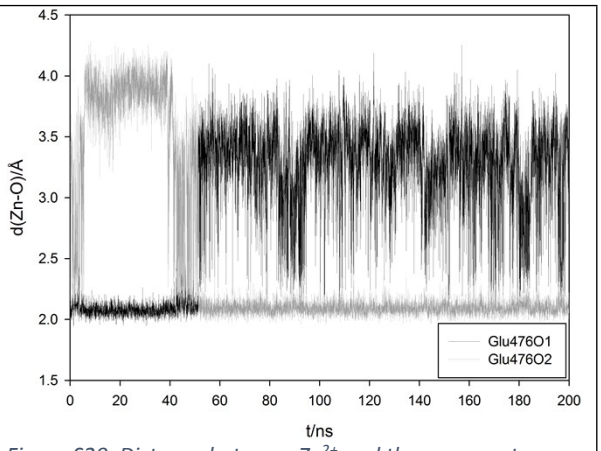

Figure S20. Distance between Zn^{2+} and the oxygen atoms of coordinating Glu476 residues over the course of 200 ns simulations of BtDPP III – RRNA complex using ff12SB force field

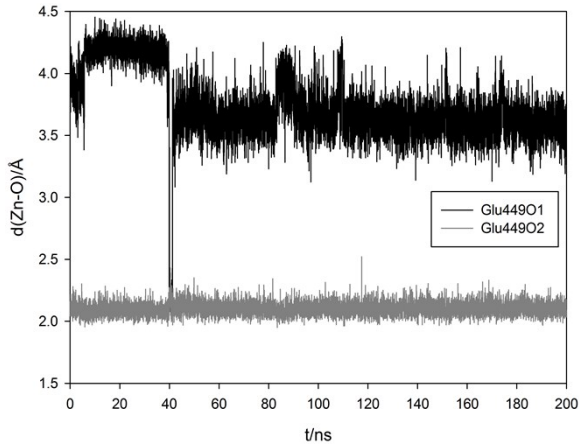

Figure S21. Distance between Zn^{2+} and the oxygen atoms of coordinating Glu449 residues over the course of 200 ns simulations of BtDPP III – RRNA complex using ff12SB force field

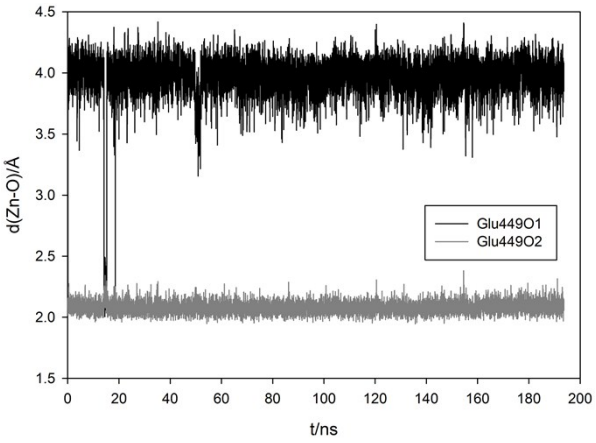

Figure S22. Distance between Zn^{2+} and the oxygen atoms of coordinating Glu449 residues over the course of 200 ns BtDPP III – RRNA complex using ff14SB force field and accelerated MD

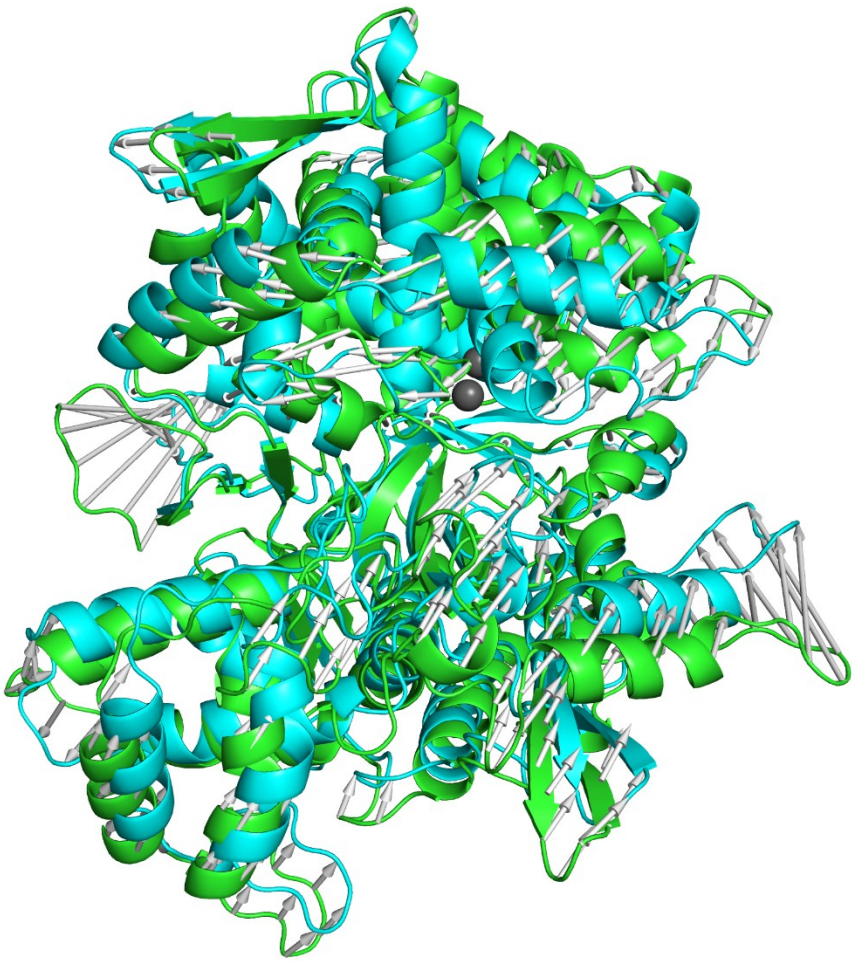

Figure S23. Difference in domain orientation in cWT and WT_{MD} structures. cWT is shown in blue, while WT_{MD} is shown in green.

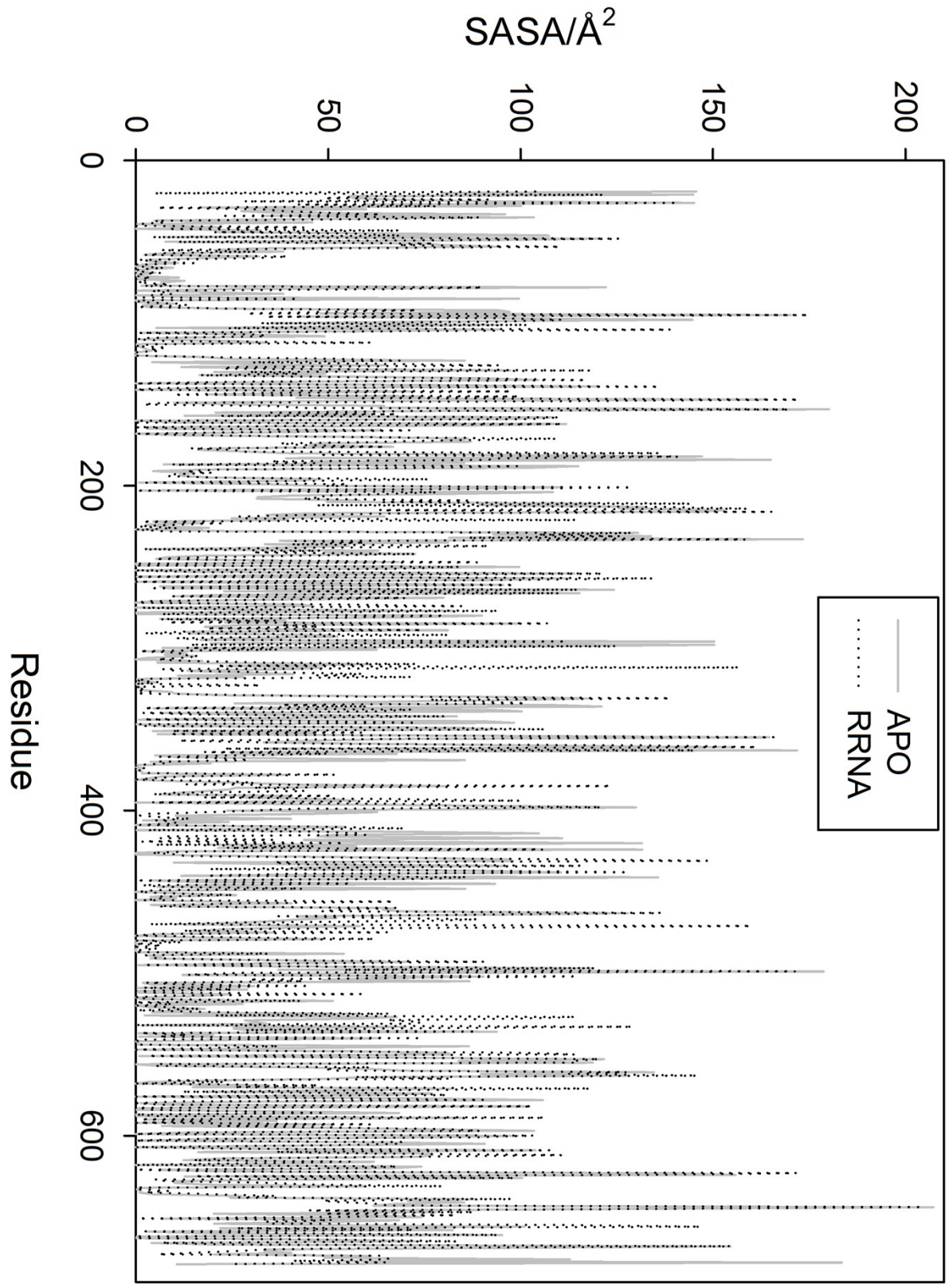

Figure S24. SASA of the residues in ligand-free DPP III and the DPP III-RRNA complex at the end of the 200 ns ff12SB cMD simulations

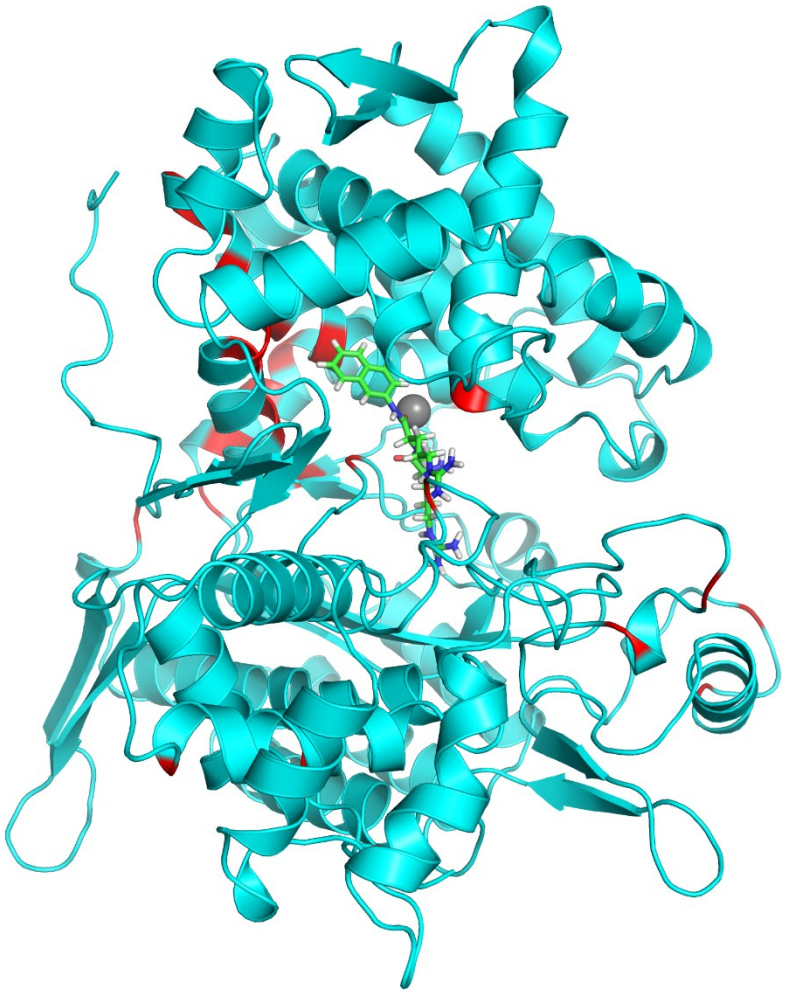

Figure S25. BtDPP III - RRNA complex. Residues with largest al-atom SASA difference from apo form are shown red.

Table S1. Overview of simulations performed in this work. Complexes of BtDPP III simulated with ff14 aMD were subsequently simulated for another 100 ns using ff12cMD for energy comparison

System	Force field	Type of simulation	Simulation duration
*Bt*DPP III	ff03	cMD	200
*Bt*DPP III	ff12SB	cMD	200
*Bt*DPP III	ff14SB	cMD	200
*Bt*DPP III	ff14SB	aMD	200
*Bt*DPP III + RRNA	ff12SB	cMD	200
*Bt*DPP III + RRNA	ff14SB	aMD	200
*Bt*DPP III + RRNA	ff12SB	cMD	100
*Bt*DPP III + KANA	ff14SB	aMD	100

Table S2. Values of geometric parameters used to describe the degree and type of BtDPP III closure determined in the most distinct enzyme structures. The radius of gyration (Rg) was calculated for the protein backbone atoms

geometric parameters	cWT	*Bt*DPP III			*Bt*DPP III - RRNA		*Bt*DPP III - KANA	
		cMD ff03	cMD ff12SB	cMD ff14SB	cMD ff12SB	aMD ff14SB	cMD ff12SB	aMD ff14SB
R_g / Å	25	26	25	25	26	25	26	26
d_1(D193-K468) / Å	24	31	21	27	29	27	29	31
d_2(D208- K468) / Å	21	20	18	25	21	18	25	25
d_3(A394- K468) / Å	23	15	17	15	19	17	18	15

Table S3. Hydrogen bonds population (%). The analysis was performed for the last 100 ns of the 200 ns long trajectory of the BtDPP III – RRNA complex using ff12SB force field. Hydrogen bonds present in <1% of the sampled structures are omitted.

Acceptor	RRNA	Donor	% of frames
∑His119	42.31	Ile382	2.71
Thr306	1.38	Gly383	28.96
∑Glu307	68.47	Asn385	-
∑Glu320	135.22		
∑Gly383	18.25		
∑Glu449	4.37		
∑Glu476	84.47		
∑Glu531	96.86		

Table S4. The MM-PBSA and MM-GBSA energies calculated for the BtDPP III-RRNA and BtDPP III -KANA complexes.

Complex	Method	$\Delta E_{MM\text{-}PBSA}$ /kcalmol^{-1}	SD/ kcalmol^{-1}	$\Delta E_{MM\text{-}GBSA}$ /kcalmol^{-1}	SD/ kcalmol^{-1}
DPP III – RRNA	cMD-ff12SB	-15.39	11.58	-23.19	8.04
DPP III – KANA	cMD-ff12SB	-13.75	7.80	-27.33	4.38
DPP III – RRNA	aMD-ff14SB	-10.59	7.95	-24.52	5.61
DPP III – KANA	aMD-ff14SB	-7.09	5.40	-21.68	5.26

Table S5. The MM-GBSA energies calculated for the Bt*DPP III-RRNA and* Bt*DPP III -KANA complexes. All energies are given in kcalmol^{-1}*

	ff12SB	ff14SB aMD
RRNA	-29.40 ± 2.23	-29.04 ± 2.47
KANA	-28.77 ± 2.03	-26.63 ± 1.79

Table S6. The MM-PBSA energies calculated for the wild-type BtDPP III and C450S BtDPP III -RRNA complexes.

Complex	Method	$\Delta E_{MM\text{-}PBSA}$ /kcalmol^{-1}	SD/ kcalmol^{-1}	$\Delta E_{MM\text{-}GBSA}$ /kcalmol^{-1}	SD/ kcalmol^{-1}
wt-DPP III	cMD-ff12SB	-15.39	11.58	-23.19	8.04

C450S DPP III	cMD-ff12SB	-9.25	8.53	-17.58	6.17
wt-DPP III	aMD-ff14SB	-10.59	7.95	-24.52	5.61
C450S DPP III	aMD-ff14SB	-6.00	8.62	-27.31	7.56